Metrol. Meas. Syst., Vol. 32 (2025) No. 4, pp. 1–15
DOI: 10.24425/mms.2025.154675

PAN POLSKA AKADEMIA NAUK

METROLOGY AND MEASUREMENT SYSTEMS
Index 330930, ISSN 0860-8229
www.metrology.wat.edu.pl

M&MS

UNCERTAINTY IN THERMOLUMINESCENCE ANALYSIS: A NEW CRITERION TO ASSESS THE DECONVOLUTION PROCESS

Amr M. Sadek[1,5)], Turki S. AlQahtani[1)], Yahya Mobarki[2)], Teodoro Rivera-Montalvo[3)], Maha A. Farag[5)], George Kitis[4)]

1) General Administration of Testing Laboratories, Saudi Standards for Metrology and Quality Organization (SASO), Riyadh, Kingdom of Saudi Arabia (✉ *a.sadek @saso.gov.sa*).
2) Nuclear and Radiological Regulatory Commission (NRRC), Riyadh, Kingdom of Saudi Arabia.
3) Research Center in Applied Science and Advanced Technology-Legaria, IPN, Ciudad de Mexico, Mexico.
4) Aristotle University of Thessaloniki, Department of Physics, Section of Nuclear Physics and Elementary Particle Physics, Thessaloniki, Greece.
5) Department of Metrology of Ionizing Radiation, National Institute for Standards (NIJS), Giza, Egypt.

Abstract

For decades, the deconvolution analysis of the thermoluminescence glow curve has been assessed using the figure of merit (FOM). In the present study, it has been shown that the FOM is not sufficient to assess the deconvolution analysis of TL glow curves. An alternative criterion has been proposed based on the uncertainty of the deconvolution analysis. A comparison between the proposed criterion and the FOM was conducted using theoretical simulations and experimental results. It has been shown that the developed criterion can provide detailed information about the fitting quality for each region in the glow curve as well as give an overall assessment of the deconvolution process. The uncertainty of deconvolution analysis using the general-order kinetics has been estimated for various glow curves. The TL-SDA toolkit has been updated to include the feature of evaluating the uncertainty of the deconvolution process.

Keywords: Evaluation of Uncertainty, Thermoluminescence, Glow Curve Analysis.

1. Introduction

Thermoluminescence (TL) is a phenomenon of luminescence emitted] from insulators or semiconductor materials when subjected to thermal stimulation. The TL phenomenon can be explained in the light of the energy band theory of solids as illustrated by Fig. 1.

TL emission is the result of a TL material subjected to irradiation process and thermal excitation. During irradiation, the electrons in the valence band are excited by the radiation energy to the conduction band. The free electrons in the conduction band have the probability of being trapped by a site of crystalline imperfection called the trapping state [1]. If thermal excitation is sufficient, the trapped electrons are released to the conduction band where they have a probability to recombine with holes at some sites, which is called the recombination state [2]. When trapped electrons are recombined with luminescence centre, TL signals are emitted [3].

Article history: received March 14, 2025; revised 8, 2025; accepted May 30, 2025; available online July 9, 2025.

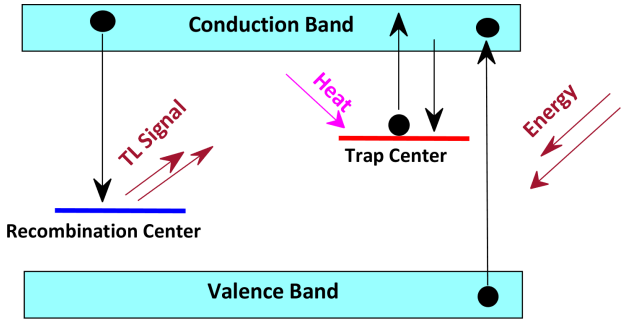

Fig. 1. Energy band gap model showing electronic transition in a TL material.

TL emission versus excitation temperature or time is called a TL glow curve, which usually consists of some peaks. Each peak represents a trap type with a defined trap depth, called activation energy E. The area under the glow curve is proportional to the concentration of electrons trapped during the irradiation process [1]. From this point, it was proposed to use TL materials for radiation dosimetric purposes [4].

Prior to using a TL detector, it must be subjected to a calibration process in which the TL responses are calibrated to radiation doses. Linear TL dose-response is preferred in dosimetric applications. However, several factors, including background noise signals, scattering data, and nonlinear signals included in the TL glow curve, can affect the accuracy of TL measurements [5, 6]. Therefore, experimental techniques [7], theoretical approaches, and artificial intelligence technology [8] were developed to improve the TL dose measurements. However, the deconvolution analysis of TL glow curves is one of several techniques proposed to separate the dosimetric peak from redundant signals [9]. Indeed, various dosimetric applications are based on the TL technique [10–12]. Furthermore, some applications demonstrate analysing the TL spectrum with respect to its individual components [13–17]. However, deconvolution analysis was also used to estimate the characteristics of TL detectors [17–24].

Unfortunately, deconvolution analysis is tricky due to the great diversity of TL glow curves [26]. A complex structure glow curve may have different solutions in deconvolution analysis [27]. Furthermore, no criteria can clearly identify the optimal solution. However, it is often necessary to assess the deconvolution analysis of TL glow curve using the *Figure of Merit* (FOM) [28], which is defined as:

$$\mathrm{FOM}\,(\%) = \sum_i \frac{|I_i\,(\mathrm{Experimental}) - I\,(\mathrm{Fit})|}{A} \times 100. \tag{1}$$

The FOM is based on comparing the summation of absolute differences between the experimental results and model estimations normalized to the area under the curve A. A general criterion demonstrates a FOM $< 2.5\%$ for satisfactory fitting [28]. At the same time, a threshold of FOM $<$ 5.0% was set by Horowitz and Yossian [9] who concluded that the FOM threshold should consider the number of analysed glow peaks. In other words, a threshold of 5% for a glow curve deconvolution of multiple peaks is less satisfactory than that for a glow curve deconvolution of a single peak.

The low values of the FOM do not necessarily imply that the model could interpret the data. In fact, the representation of the model to the data is always suspected if information regarding the uncertainties of the model's parameters and their effect on the output of the model the is not available [29].

In TL science, there are mainly three models developed to describe the TL glow peak. The first- and second-order kinetic models [30, 31] describe the TL glow peak as a function of the initial

concentration of trapped electrons n_0, the activation energy E, and the frequency factor s. Also, general- and mixed-order kinetic models [32, 33] used additional parameters, namely the kinetic order b and mixed-order α, respectively. Later, Kitis *et al.* [34] deduced the first, second-, and general-order kinetic model equations by replacing the parameters n_0 and s with the peak maximum I_m and peak maximum position T_m which can be obtained from an experimental glow curve.

Various software applications were developed to deconvolute the TL glow curves. A list of these software applications was provided by Peng *et al.* [35], who developed a software application to analyse the TL spectrum using various models. Recently, Sadek *et al.* [36] have developed a TLSDA toolkit that can run using MATLAB. The advantage of this application is that it can deconvolute complex structure glow curves without the need to perform several trials. Furthermore, there is no need to have prior knowledge of the number of TL peaks or the activation energy. Nevertheless, none of these software applications provides an uncertainty for the fitting model used in the deconvolution analysis process. Therefore, the main aims of the present work are:

1. Develop a new criterion to assess the deconvolution analysis of the TL glow curve based on the uncertainty of the TL model.
2. Compare the new criterion with the default FOM.
3. Release a new version of the TLSDA toolkit [36] to include the evaluation of the uncertainty of the TL deconvolution analysis process.

2. Methodology of evaluation of uncertainty

The evaluation of uncertainty of the fitting model used in the deconvolution analysis process was performed following the *Joint Committee for Guides in Metrology* (JCGM) guide [37, 38]. The JCGM methodology is based on both Bayesian probabilistic methods [39], as well as classical probabilistic methods [40]. Assuming that the error is propagated through the output system, the method evaluates the uncertainty associated with each source of error affecting the output system. Then, these sources of uncertainty are combined into a single value.

In least-squares problems, the uncertainty of the output model is a combination of the uncertainty components associated with the parameters of the model [41, 42]. In TL, the *general-order kinetics* (GOK) model equation describes the TL signal assuming a single glow peak by a mathematical representation of 5 parameters as [43]:

$$I(E, s, n_0, b|T) = n_0 s e^{-\frac{E}{kT}} \left[\frac{s\,(b-1)}{\beta} F(T, E) + 1 \right]^{-\frac{b}{b-1}}, \tag{2}$$

where:

$$F\,(T, E) = \int_{T_0}^{T} \exp\left(-\frac{E}{kT}\right) \mathrm{d}T. \tag{3}$$

It implies that the uncertainty of the model output is a combination of the uncertainty components associated with n_0, E, sb and β. The combined associated standard uncertainty can be estimated by [37]:

$$u\,(I) = \sqrt{\sum_i \left(v_i^I u_i\right)^2 + 2 \sum_i \sum_j c_i c_j u_i u_j r\,(i, j)}, \tag{4}$$

where v_i is the sensitivity coefficient that represents the impact of the uncertainty component i on the final measured quantity [44, 45], u_i is the associated standard uncertainty, and $r\,(i, j)$ is the correlation coefficient between the uncertainty components i and j, which is sometimes a crucial factor [46].

The sensitivity coefficient associated with the uncertainty components is evaluated as [37]:

$$v\left(n_0\right)=\frac{\partial I}{\partial n_0}=s\,e^{-\frac{E}{\mathrm{kT}}}\left[\frac{s\left(b-1\right)}{\beta}F\left(T,E\right)+1\right]^{-\frac{b}{b-1}}, \tag{5}$$

$$v\left(E\right)=\sigma_2\left\{\sigma_1+Tbs\left(Ei\left[-\frac{E}{\mathrm{kT}}\right]-Ei\left[-\frac{E}{\mathrm{kT}_0}\right]\right)\right\}, \tag{6}$$

$$v\left(s\right)=\frac{n_0\beta e^{-\frac{E}{\mathrm{kT}}}}{\sigma_1^2}\left(\beta-s\,F\left(T,E\right)\right)\left(\frac{\sigma_1}{\beta}\right)^{\frac{-1}{b-1}}, \tag{7}$$

$$v\left(b\right)=n_0 s\,e^{-\frac{E}{\mathrm{kT}}}\left(\ln\left(\frac{\sigma_1}{\beta}\right)\frac{\left(\frac{1}{b-1}-\frac{b}{(b-1)^2}\right)}{\left(\frac{\sigma_1}{\beta}\right)^{\frac{b}{b-1}}}+\frac{bsF\left(T,E\right)}{\beta\left(b-1\right)\left(\frac{\sigma_1}{\beta}\right)^{1+\left(\frac{b}{b-1}\right)}}\right), \tag{8}$$

$$\sigma_1=\beta+s\,F\left(T,E\right)\left(1-b\right),\ \sigma_2=-\frac{\beta n_0 s e^{-\frac{E}{\mathrm{kT}}}}{kT\sigma_1\left(\frac{\sigma_1}{\beta}\right)^{\frac{1}{b-1}}}. \tag{9}$$

Ei is a one-argument exponential integral function. In the deconvolution of the experimental glow curve, the TL expression deduced as a function of the peak maximum I_m and peak maximum position T_m by Kitis *et al.* [34] is used.

$$I\left(I_m,T_m,E,b\,|\,T\right)=I_m e^{-\frac{E}{\mathrm{k}}\frac{TT_m}{T+T_m}}\frac{\left(\frac{b}{\sigma_3}\right)^{\frac{b}{b-1}}}{\left(\frac{Ee^{\frac{E}{kT_m}}\left(b-1\right)}{kT_m^2\sigma_3}F\left(T,E\right)+1\right)^{\frac{b}{b-1}}}, \tag{10}$$

where:

$$\sigma_3=\frac{2kT_m\left(b-1\right)}{E}+1. \tag{11}$$

The effect of each uncertainty component on the output TL signal is illustrated in Fig. 2. It is worth noting that the uncertainty components are a function of temperature. The uncertainty component associated with the activation energy E is dominant compared to the other sources of uncertainties. Furthermore, the parameter E is correlated with T_m through the peak maximum conditions. This correlation is accounted for in the evaluation of uncertainty by the correlation coefficient $r\left(E,T_m\right)$.

The assessment of the deconvolution process allows us to express the combined standard uncertainty evaluated at each channel $\{T_i,I\left(T_i\right)\}$ as:

$$u_c\left(I\right),\,\%=\sum_i\frac{u_c\left\{I\left(T_i\right)\right\}}{I\left(T_i\right)}\times 100, \tag{12}$$

where $u_c\left\{I\left(T_i\right)\right\}$ is the combined standard uncertainty evaluated at channel i. This standard uncertainty should be investigated over the temperature range of a TL glow curve to illustrate the regions of high uncertainty values, and thereby, low performance of the model. On the other hand, the parameter u_c describes the uncertainty of the entire deconvolution analysis process. By investigating the u_c parameter, a general criterion for satisfactory deconvolution analysis can be established.

Metrol. Meas. Syst., Vol. 32 (2025), No. 4, pp. 1–15
DOI: 10.24425/mms.2025.154675

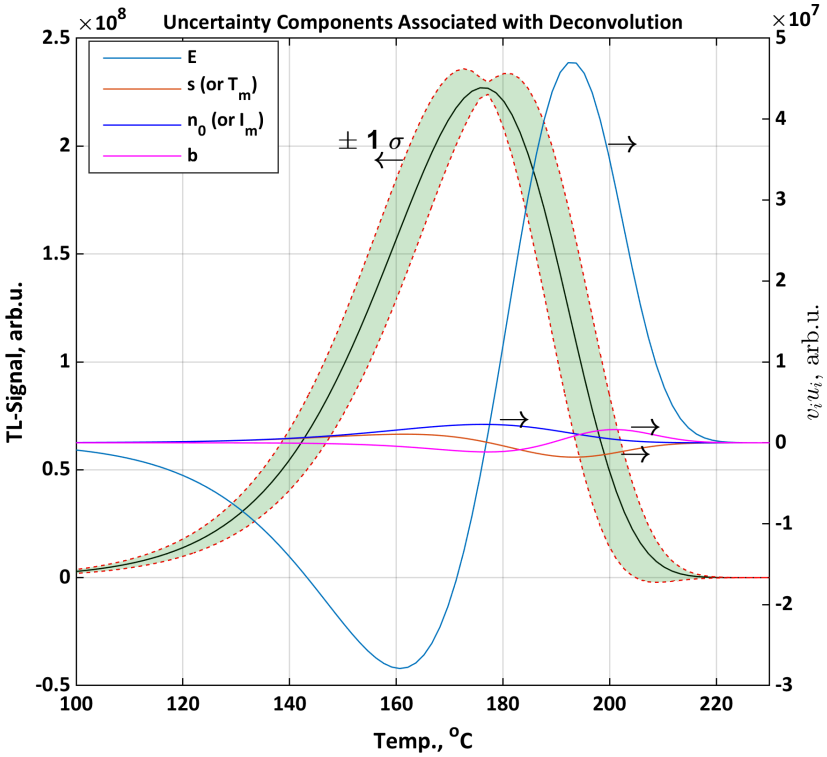

Fig. 2. Effect of each uncertainty component on final TL signal evaluated by deconvolution analysis.

3. Factors affecting the uncertainty of the deconvolution process

In the present section, the factor affecting the deconvolution analysis of a TL glow curve has been investigated throughout theoretical simulations. The glow curve was simulated using the *noninteractive multiple-trap system model* (NMTS), where the electron transitions among the states are described as:

$$\frac{\mathrm{d}n_i}{\mathrm{d}t} = -n_i s\, e^{-\frac{E_i}{kT}} + n_c\,(N_i - n_i)\,A_i, \quad \text{for } i = 1, 2, ..l, \tag{13}$$

$$\frac{\mathrm{d}n_c}{\mathrm{d}t} = \sum_{i=1}^{l}\left[n_i s\, e^{-\frac{E_i}{kT}} - n_c\,(N_i - n_i)\,A_i\right] - n_c m A_m, \tag{14}$$

$$\frac{\mathrm{d}m}{\mathrm{d}t} = -n_c m A_m, \tag{15}$$

where $\mathrm{d}n_i/\mathrm{d}t$ describes the change in the electron concentrations $n\,(t)$ in trapped in the trapping states N_i with trapping probability coefficients A_i. The $\mathrm{d}m/\mathrm{d}t$ describes, on the other hand, the change in concentration of recombination states $m\,(t)$ of recombination probability coefficient A_m. The $\mathrm{d}n_c/\mathrm{d}t$ describes the electron transitions among the trapped and recombination states through the conduction band.

3.1. Effect of overlapping between peaks

Critical arguments were proposed that CGCD cannot yield reliable trap parameters, and deconvolution analysis cannot reach a global minimum for glow curves of overlapping peaks [47,48]. Therefore, Kierstead and Levy [49] reported that the CGCD is reliable if the glow peaks are well separated. Unfortunately, the FOM does not provide information about the complexity of the TL spectrum. However, using the uncertainty criterion, information about the complexity of the TL glow curve and the region where the model could not interpret the data can be provided.

Figure 3 presents a glow curve of four glow peaks simulated using the NMTS model. The trapping parameters were selected so that two glow peaks overlap, and the other two peaks are separated. The FOM indicated a satisfactory fitting. The relatively high values of u_c over temperature indicate overlapping between peaks. However, the final u_c (%) may still indicate an acceptable overall deconvolution analysis.

The experimental data in the GLOCANIN project [50] included glow curves of LiF:Mg,Ti detectors subjected to various experimental conditions. It should be noted that in addition to precision, there are several Type-B uncertainty sources that affect the TL emission, including the TL calibration curve, batch homogeneity, source of radiation, TL reader stability, and fading correction. Evaluations of these sources were addressed by Sadek et al [51] and found to be at the level of 4.5% [1σ] for LiF:Mg,Ti detectors and the Harshaw 3500 TL system. This level of uncertainty may vary depending on the type of the TL detector used and the TL reader system.

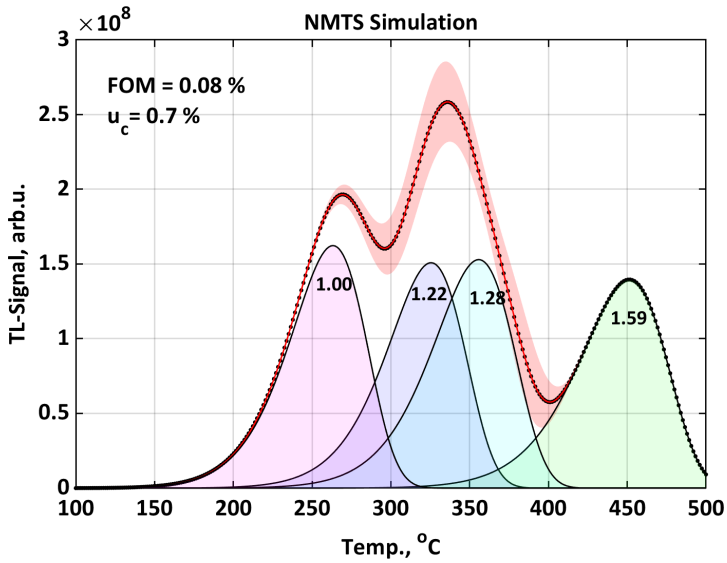

Fig. 3. Deconvolution performed for the glow curve simulated using the NMTS model with overlapping peaks. The activation energy obtained by the deconvolution analysis is denoted in eVs at the maximum of each peak. The quality of the fitting was assessed using the default FOM and new $\boldsymbol{u_c}$ criteria.

For dosimetric applications, where the peak maximum or peak integral estimated from the deconvolution analysis is used, Type-B uncertainty should be considered in the evaluation of the combined standard uncertainty to ensure a reasonable uncertainty assessment. In fact, accounting for Type-B uncertainty improves the clarity and reliability of uncertainty interpretation with the deconvolution process, providing a comprehensive framework for its implementation in dosimetric applications.

RefGC#09 represents a glow curve of an LiF:Mg,Ti detector irradiated with high gamma dose levels. However, the deconvolution analysis of the high-temperature glow peaks of this curve is still a challenge because they overlap. The glow curves of LiF:Mg,Ti irradiated by heavy ions are more complicated than the glow curve of LiF:Mg,Ti irradiated with high doses [9, 52]. Therefore, in the present section these glow curves were analysed, and the analysis quality was estimated. Fig. 4 presents the deconvolution analysis of RefGC#09 and the LiF:Mg,Ti alpha irradiation glow curve [27].

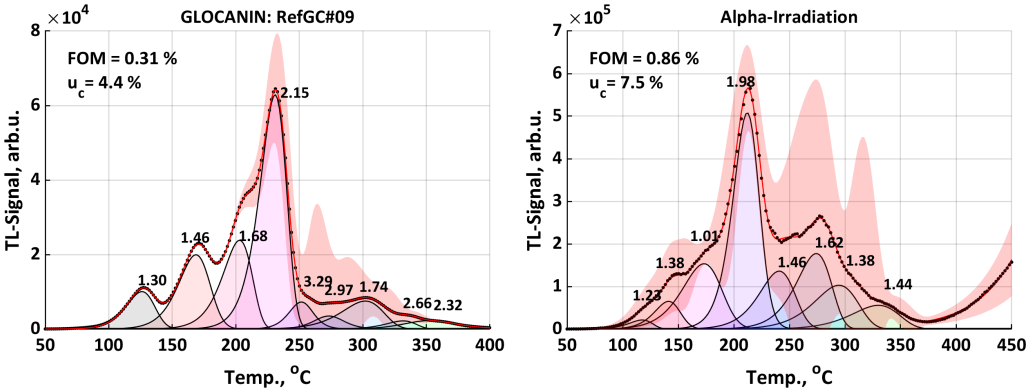

Fig. 4. Deconvolution analysis of the GLOCANIN glow curves #09 and glow-curve of LiF:Mg,Ti irradiated with alpha particles. The activation energy obtained from the deconvolution analysis is denoted in eVs for the maximum of each peak. The deconvolution analysis was assessed using the FOM and u_c criteria.

The FOM in both cases of Fig. 5 indicated a satisfactory fit, while high u_c values were obtained. By investigating the u_c over the temperature range for the TL glow curve, one finds that the deconvolution analysis of the high temperature part $T > 250°C$ of RefGC#09 suffers from higher uncertainty values. For the alpha-irradiation case, high uncertainty values were obtained for the model all over the temperature range. These high uncertainty values are due to the complex structure of the glow curve. This implies that the deconvolution analysis would have many other possible solutions.

The above discussion reveals that the FOM does not provide information on the complexity of the TL spectrum. Furthermore, it may provide an unrealistic assessment for the deconvolution of overlapping glow peaks. On the other hand, it shows the importance of investigating the model performance over the temperature range of the TL spectrum along with the final uncertainty criterion u_c.

3.2. Effect of data size

The TLD reader systems record the temperature and the corresponding TL intensity over a predefined channel number. In Harshaw 4500 and 3500 TLD reader systems, the temperature and TL intensity are recorded over 200 channels regardless of the temperature profile settings. However, some other TLD reader systems can record the TL glow curve over 1000 channels [2].

Typically, increasing the channels size should improve the fitting quality and increase the reliability of the model's prediction [53]. To investigate the effect of the size of channels on the fitting model performance, glow peaks were simulated with different channel sizes using the NMTS model. In each case, the peak was fitted by the GOK expression, and the fitting quality parameters were estimated. In the TLSDA software [36], the fitting quality was assessed through the FOM, root mean square of error (RMSE), and R − Square, where:

$$\text{R} - \text{Square} = 1 - \frac{\text{SSE}}{\text{SST}}, \tag{16}$$

$$\mathrm{SSE} = \sum_{i=1}^{Chn} \left(y_i - y\left(x_i\right)\right)^2, \quad \mathrm{SST} = \sum_{i=1}^{Chn} \left(y_i - \overline{y}\right)^2, \tag{17}$$

$$\mathrm{RMSE} = \sqrt{\frac{\mathrm{SSE}}{v}}, \tag{18}$$

where Chn is the channel size, and v is the degree of freedom $v = Chn - 1$. Fig. 5 presents the goodness-of-fit parameters of fitting a TL glow peak simulated by the NMTS model with different channel sizes.

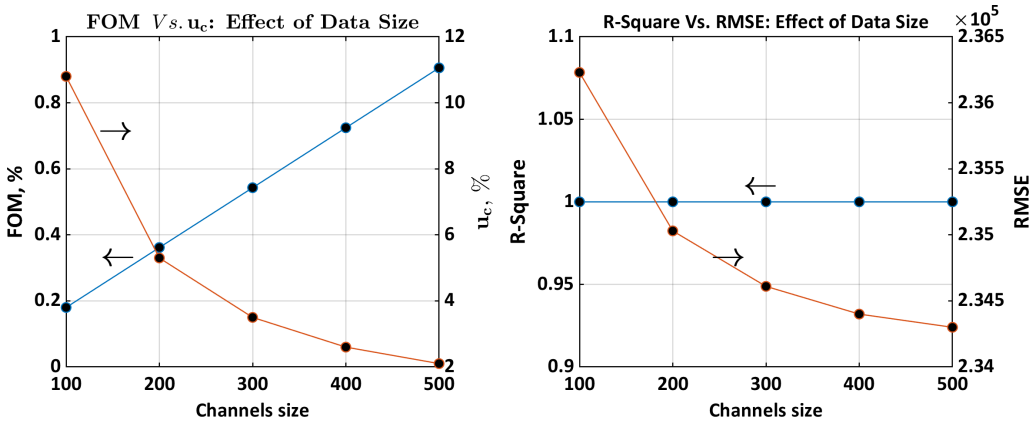

Fig. 5. Comparison between the evaluation of goodness of fitting using FOM and uncertainty over various channel sizes.

High FOM values were obtained when the number of channels increased. These high FOM values are attributed to the term of $\sum_i I\,(\text{experimental}) - I\,(\text{Fit})$ in the FOM expression which increases with increasing channel size. On the other hand, the u_c criterion showed that the performance of the fitting model was improved as the data size increased. This improvement in the model's performance was also confirmed by the fitting quality parameters. The $RMSE$ parameter is similar to the FOM, except it evaluates the average of the square of the model's error instead of normalizing it to the curve area. Therefore, it eliminates the effects of changing the channel size. The $R - Square$ also eliminates the effect of channel size by the ratio of SSE/SST which takes the average $\overline{y}$ into account.

The Lexsyg Smart TL/OSL reader system can record TL glow curves with different channel sizes by varying the heating rates over the same temperature range. A set of TL glow curves of $GdAlO_3$ detectors exposed to 13.2 Gy beta irradiation were recorded with different channel sizes. The deconvolution analyses of these curves are illustrated in Fig. 6.

It was observed that at large channel sizes, the uncertainty of the fitted curve was minimum. However, as the channel size decreased, the uncertainty of the fitted curve increased, especially in the temperature region where the glow peaks overlapped. In contrast, the FOM increased with increasing channel size, as illustrated in Fig. 7.

It was observed that the FOM is very sensitive to the channel size of the temperature readout. In fact, the FOM may reach an unacceptable level because of the large channel size. This illustrates the advantage of using the uncertainty of the fitted curve as a parameter of goodness of fitting quality instead of the FOM in these cases. This implies that the FOM may provide unreasonable assessment for the deconvolution analysis of TL spectrums that were recorded with large channel sizes.

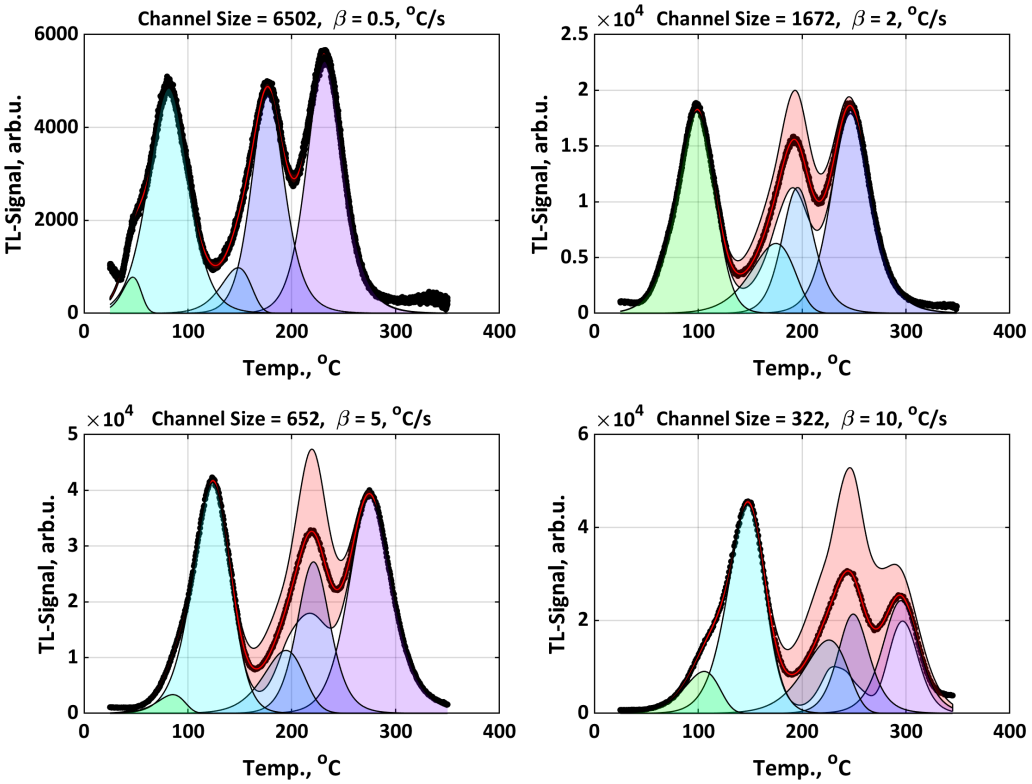

Fig. 6. Deconvolution analysis of a set of glow curves recorded with different channel sizes.

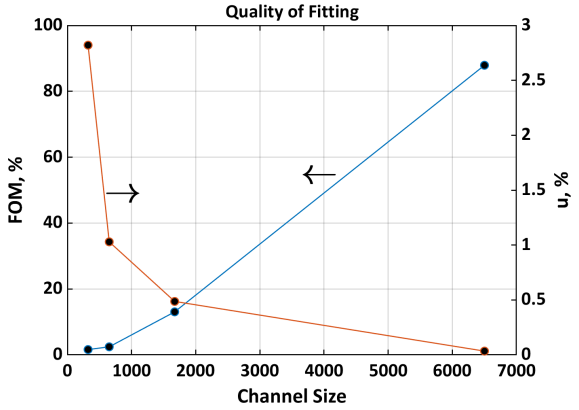

Fig. 7. FOM and uncertainty of the fitting curve over the channel size of the temperature readout.

3.3. Effect of scatter data

The effect of scatter data on the evaluation of the TL dose-response curve was previously investigated [5, 6]. In these studies, the scatter data was simulated following the Monte-Carlo algorithm [38] where random error E was induced to each data point of TL intensity. In other

words, for a data point x, the scattering effect can be induced as:

$$\xi = x + a\,(x)\,z,\; E = \xi - x, \tag{19}$$

where $a\,(x)$ is adjustable standard error and z is standard normal distribution of mean 0 and standard deviation 1. In the present study, $a\,(x)$ was introduced as a fraction of maximum peak intensity. Figure 8 illustrates the effect of the scatter data on the fitting quality and uncertainty estimation of a single glow peak.

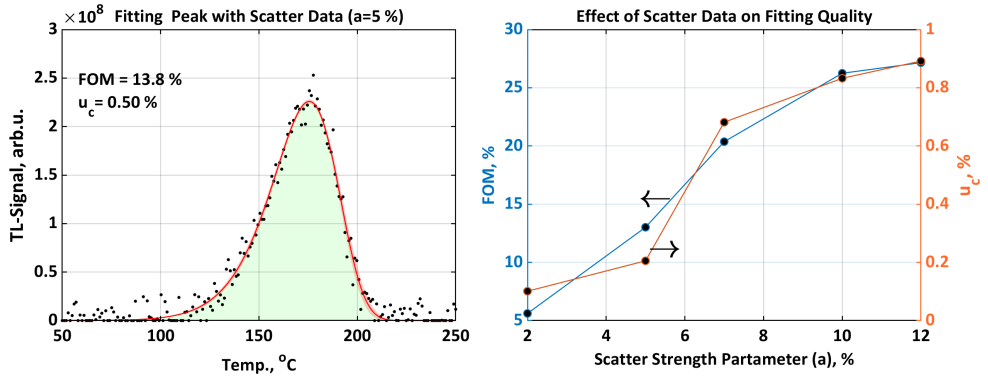

Fig. 8. Effect of scatter data on the quality of fitting and model's uncertainty estimations.

At $a = 5\%$, a high $FOM = 13.8\%$ value indicating unsatisfactory fitting was obtained. The high FOM values are due to the high dispersion of the scatter data appearing at the low- and high-temperature tails of the peak. On the other hand, $u_c = 0.5\%$ was obtained referring to a successful fit. It is successful because the entire range of the single glow peak was fitted by the model, and therefore, it was able to determine the trapping parameters with an acceptable precision. Nevertheless, this may not be the case with experimental data.

Scatter data is usually observed in the case of low dose levels. The RefGC#10 of the GLOCANIN project represents the glow curve of a LiF:Mg,Ti detector irradiated by 0.2 mGy. The deconvolution analysis of RefGC#10 is presented in Fig. 9.

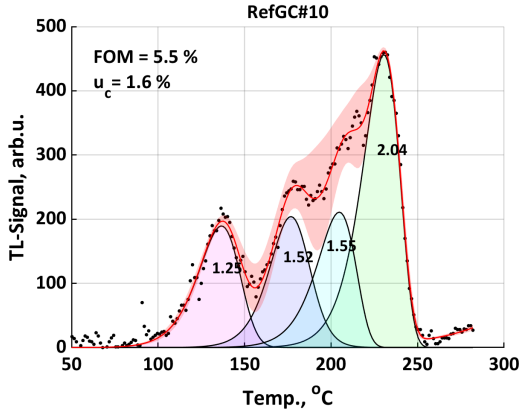

Fig. 9. Deconvolution analysis of GLOCANIN RefGC#10. The activation energy obtained from the deconvolution analysis is denoted in eVs at the maximum of each peak. The deconvolution analysis was assessed using the FOM and u_c criteria.

High FOM and u_c values were estimated for RefGC#10. These high values are attributed to the scatter data in the TL signal. It is worth noting that the uncertainty u_c over the temperature range of glow curve increases in the area where the peaks overlap. This is because in these regions the uncertainty of TL signals is affected by both the scatter data and the overlapping effect. On the other hand, it reveals that overlapping between peaks is dominant compared to the scatter data.

4. Conclusions

Critical drawbacks have been observed when using the FOM criterion to assess the deconvolution analysis of TL glow curves. The FOM may not provide reasonable assessment for the deconvolution analysis of TL glow curves when the glow peaks overlap. Furthermore, it provides a misleading assessment for the deconvolution analysis of glow curves recorded with a large channel size. These disadvantages can be overcome with the proposed assessment criterion based on the uncertainty of the deconvolution process.

The developed uncertainty criterion can provide detailed information about the performance of the fitting model at each region in the glow curve. In this way, the use of the TL signals in regions where the uncertainty is high can be subjected to further investigation or used with caution. On the other hand, it can also provide an overall assessment for the deconvolution process of the TL glow curve.

References

[1] Vij, D. R. (1998). Luminescence of Solids. In *Springer eBooks*. https://doi.org/10.1007/978-1-4615-5361-8

[2] Furetta, C. (2003). *Handbook of Thermoluminescence*. https://doi.org/10.1142/9789812564863

[3] Bos, A. (2006). Theory of thermoluminescence. *Radiation Measurements*, *41*, S45–S56. https://doi.org/10.1016/j.radmeas.2007.01.003

[4] Daniels, F., Boyd, C. A., & Saunders, D. F. (1953). Thermoluminescence as a research tool. *Science*, *117*(3040), 343–349. https://doi.org/10.1126/science.117.3040.343

[5] Sadek, A., Pagonis, V., & Kitis, G. (2020). Influence of scatter data and temperature lag on the analysis of thermoluminescence glow peak: A Monte Carlo simulation study. *Applied Radiation and Isotopes*, *167*, 109405. https://doi.org/10.1016/j.apradiso.2020.109405

[6] Sadek, A. M. (2020). Uncertainty of thermoluminescence at low dose levels: A Monte-Carlo simulation study. *Radiation Protection Dosimetry*, *192*(1), 14–26. https://doi.org/10.1093/rpd/ncaa177

[7] Armstrong, P., Mah, M., Ross, H., & Talghader, J. (2018). Individual microparticle measurements for increased resolution of thermoluminescent temperature sensing. *IEEE Sensors Journal*, *18*(11), 4422–4428. https://doi.org/10.1109/jsen.2018.2823678

[8] Amit, G., Vagerman, R., & Revayev, O. (2024). 'TLDetect': AI-Based application for detection and correction of anomalous TLD glow curves. *Sensors*, *24*(21), 6904. https://doi.org/10.3390/s24216904

[9] Horowitz, Y. S., & Yossian, D. (1995). Computerised glow curve deconvolution: Application to thermoluminescence dosimetry. *Radiation Protection Dosimetry*. https://doi.org/10.1093/oxfordjournals.rpd.a082702

[10] Mandowska, E., Smyka, R., & Mandowski, A. (2023). Investigating the filling state of OSL detector traps with the optical sampling method. *Metrology and Measurement Systems*. https://doi.org/10.24425/mms.2022.140039

[11] Sandeva, I., Spasevska, H., Ginovska, M., & Stojanovska-Georgievska, L. (2017). Effects of radiation doses on the photostimulated luminescence response of certain herbs and spices. *Metrology and Measurement Systems*, *24*(1), 143–151. https://doi.org/10.1515/mms-2017-0003

[12] Mihóková, E., & Nikl, M. (2014). Luminescent materials: probing the excited state of emission centers by spectroscopic methods. *Measurement Science and Technology*, *26*(1), 012001. https://doi.org/10.1088/0957-0233/26/1/012001

[13] Fuks, E., Horowitz, Y. S., Horowitz, A., Oster, L., Marino, S., Rainer, M., Rosenfeld, A., & Datz, H. (2010). Thermoluminescence solid-state nanodosimetry – the peak 5A/5 dosemeter. *Radiation Protection Dosimetry*, *143*(2–4), 416–426. https://doi.org/10.1093/rpd/ncq479

[14] Horowitz, Y. S., Oster, L., Reshes, G., Nemirovsky, D., Ginzburg, D., Biderman, S., Bokobza, Y., Sterenberg, M., & Eliyahu, I. (2022). Recent developments in computerised analysis of thermoluminescence glow curves: software codes, mechanisms and dosimetric applications. *Radiation Protection Dosimetry*, *198*(12), 821–842. https://doi.org/10.1093/rpd/ncac147

[15] Sen, M., Shukla, R., Pathak, N., Bhasin, V., Jha, S. N., Bhattacharyya, D., Sathian, V., Chaudhury, P., & Tyagi, A. K. (2023). Al5BO9:Tb3+: Synthesis, structural characterization and thermoluminescence dosimetry studies for high intensity thermal neutron beams. *Ceramics International*, *49*(20), 33358–33368. https://doi.org/10.1016/j.ceramint.2023.08.051

[16] Khandaker, M. U., Nawi, S. M., Lam, S., Sani, S. A., Islam, M. A., Islam, M., Naseer, K., Osman, H., & Bradley, D. (2023). Thermoluminescent characterization and defect studies of graphite-rich media under high dose neutron exposure. *Applied Radiation and Isotopes*, *196*, 110771. https://doi.org/10.1016/j.apradiso.2023.110771

[17] Łepkowska, J., & Jung, A. (2022). Influence of readout conditions on the thermoluminescence properties of mobile phone display glass for retrospective dosimetry. *Measurement*, *204*, 112083. https://doi.org/10.1016/j.measurement.2022.112083

[18] Avci, H., Oglakci, M., Bulcar, K., & Alma, M. (2024). An investigation on thermoluminescence properties and kinetic parameters of Çankırırock salt. *Radiation Physics and Chemistry*, *225*, 112151. https://doi.org/10.1016/j.radphyschem.2024.112151

[19] Tadros, S. M., El-Kinawy, M., Kamal, R., Saif, M., & El-Faramawy, N. (2024). Synthesis and thermoluminescence characterization of BA6Y2W3O18 perovskite nanosensors for dosimetry. *Optical Materials*, *157*, 116310. https://doi.org/10.1016/j.optmat.2024.116310

[20] Zhang, Y., Chen, M., & Yang, W. (2024). Investigation of traps in electron-irradiated sapphire: Insights from thermoluminescence and fluorescence spectrum. *Materials Science and Engineering B*, *308*, 117592. https://doi.org/10.1016/j.mseb.2024.117592

[21] Manju, N., Jain, M., Savita, N., Kumar, A., Vij, A., & Thakur, A. (2021). Unraveling Trapping Defects Distribution using Thermoluminescence in Gamma-Irradiated SrZnO2:Dy Nanophosphors. *Physica Status Solidi (A)*, *218*(12). https://doi.org/10.1002/pssa.202100063

[22] Rojas, J., Cogollo, R., & Gutiérrez, O. (2022). Analysis of the thermoluminescent glow curve of alumina matrices obtained under different sintering and cerium doped conditions. *Journal of Physics Conference Series*, *2307*(1), 012027. https://doi.org/10.1088/1742-6596/2307/1/012027

[23] Vartha, A. D., Patankar, P. R., Sahare, P. D., Sharma, L., Kachere, A. R., Kakade, P. M., Bai, B., Dhole, S. D., & Mandlik, N. T. (2024). Synthesis and thermoluminescence study of Dy3+ doped ZnAl2O4 phosphor for high-dose dosimetry application. *Journal of Radioanalytical and Nuclear Chemistry*, *333*(9), 4503–4522. https://doi.org/10.1007/s10967-024-09571-x

[24] Dani, S., Kumar, S., Singh, F., Vij, A., & Thakur, A. (2021). Probing the defects and trap distribution in MgAl2O4 nanocrystals through electron spin resonance and thermoluminescence. *Journal of Physics D: Applied Physics*, *54*(33), 335303. https://doi.org/10.1088/1361-6463/ac03ec

[25] Benabdesselam, M., Bahout, J., Mady, F., Blanc, W., Hamzaoui, H. E., Cassez, A., Delplace-Baudelle, K., Habert, R., Bouwmans, G., Bouazaoui, M., & Capoen, B. (2021). TL Properties of RE-doped and Co-doped Sol-Gel Silica Rods. Application to Passive (OSL) and Real-Time (RL) Dosimetry. *IEEE Sensors Journal*, *21*(24), 27465–27472. https://doi.org/10.1109/jsen.2021.3124602

[26] Horowitz, Y. S., & Oster, L. (2024). The thermoluminescence glow curves of LiF:Mg,Ti: characteristics and mechanisms. *Radiation Protection Dosimetry*, *200*(10), 919–937. https://doi.org/10.1093/rpd/ncae140

[27] Sadek, A. M., Hassan, M. M., Esmat, E., & Eissa, H. M. (2017). A new approach to the analysis of thermoluminescence glow-curve of TLD-600 dosimeters following Am-241 alpha particles irradiation. *Radiation Protection Dosimetry*, *178*(3), 260–271. https://doi.org/10.1093/rpd/ncx105

[28] Balian, H., & Eddy, N. W. (1977). Figure-of-merit (FOM), an improved criterion over the normalized chi-squared test for assessing goodness-of-fit of gamma-ray spectral peaks. *Nuclear Instruments and Methods*, *145*(2), 389–395. https://doi.org/10.1016/0029-554x(77)90437-2

[29] Cukier, R., Levine, H., & Shuler, K. (1978). Nonlinear sensitivity analysis of multiparameter model systems. *Journal of Computational Physics*, *26*(1), 1–42. https://doi.org/10.1016/0021-9991(78)90097-9

[30] Randall, J. T., & Wilkins, M. H. F. (1945). Phosphorescence and electron traps - I. The study of trap distributions. *Proceedings of the Royal Society of London A: Mathematical and Physical Sciences*, *184*(999), 365–389. https://doi.org/10.1098/rspa.1945.0024

[31] Garlick, G. F. J., & Gibson, A. F. (1948). The electron trap mechanism of luminescence in sulphide and silicate phosphors. *Proceedings of the Physical Society*, *60*(6), 574–590. https://doi.org/10.1088/0959-5309/60/6/308

[32] May, C. E., & Partridge, J. A. (1964). Thermoluminescent kinetics of alpha-irradiated alkali halides. *The Journal of Chemical Physics*, *40*(5), 1401–1409. https://doi.org/10.1063/1.1725324

[33] Chen, R., Kristianpoller, N., Davidson, Z., & Visocekas, R. (1981). Mixed first and second order kinetics in thermally stimulated processes. *Journal of Luminescence*, *23*(3–4), 293–303. https://doi.org/10.1016/0022-2313(81)90135-6

[34] Kitis, G., Gomez-Ros, J. M., & Tuyn, J. W. N. (1998). Thermoluminescence glow-curve deconvolution functions for first, second and general orders of kinetics. *Journal of Physics D Applied Physics*, *31*(19), 2636–2641. https://doi.org/10.1088/0022-3727/31/19/037

[35] Peng, J., Dong, Z., & Han, F. (2016). tgcd: An R package for analyzing thermoluminescence glow curves. *SoftwareX*, *5*, 112–120. https://doi.org/10.1016/j.softx.2016.06.001

[36] Sadek, A., Farag, M., El-Hafez, A. A., & Kitis, G. (2024). TL-SDA: A designed toolkit for the deconvolution analysis of thermoluminescence glow curves. *Applied Radiation and Isotopes*, *206*, 111202. https://doi.org/10.1016/j.apradiso.2024.111202

[37] *Evaluation of Measurement data – Guide to the expression of uncertainty in measurement* (JCGM 100:2008). (2008). Bureau International des Poids et Mesures. https://doi.org/10.59161/jcgm100-2008e

[38] Evaluation of Measurement data – Supplement 1 to the "Guide to the Expression of Uncertainty in Measurement" – Propagation of distributions using a Monte Carlo method (JCGM 101:2008). (2008). Bureau International des Poids et Mesures. https://doi.org/10.59161/jcgm101-2008

[39] Gelman, A., Carlin, J. B., Stern, H. S., Dunson, D. B., Vehtari, A., & Rubin, D. B. (2013). Bayesian Data Analysis. In *Chapman and Hall/CRC eBooks*. https://doi.org/10.1201/b16018

[40] Neyman, J. (1937). Outline of a theory of statistical estimation based on the classical theory of probability. *Philosophical Transactions of the Royal Society of London. Series A. Mathematical and Physical Sciences*, *236*(767), 333–380. https://doi.org/10.1098/rsta.1937.0005

[41] Han, J., Lee, K., Lee, J., Park, T. S., Oh, J., & Oh, P. (2015). New method to incorporate Type B uncertainty into least-squares procedures in radionuclide metrology. *Applied Radiation and Isotopes*, *109*, 82–84. https://doi.org/10.1016/j.apradiso.2015.11.069

[42] Wurm, M. (2021). A universal and fast method to solve linear systems with correlated coefficients using weighted total least squares. *Measurement Science and Technology*, *33*(1), 015017. https://doi.org/10.1088/1361-6501/ac32ec

[43] Yossian, D., & Horowitz, Y. (1997). Mixed-order and general-order kinetics applied to synthetic glow peaks and to peak 5 in LiF:Mg,Ti (TLD-100). *Radiation Measurements*, *27*(3), 465–471. https://doi.org/10.1016/s1350-4487(97)00007-3

[44] Allard, A., & Fischer, N. (2018). Sensitivity analysis in practice: providing an uncertainty budget when applying supplement 1 to the GUM. *Metrologia*, *55*(3), 414–426. https://doi.org/10.1088/1681-7575/aabd55

[45] Lira, I. (2016). Beyond the GUM: variance-based sensitivity analysis in metrology. *Measurement Science and Technology*, *27*(7), 075006. https://doi.org/10.1088/0957-0233/27/7/075006

[46] Malengo, A., & Pennecchi, F. (2013). A weighted total least-squares algorithm for any fitting model with correlated variables. *Metrologia*, *50*(6), 654–662. https://doi.org/10.1088/0026-1394/50/6/654

[47] Sakurai, T. (2001). Fatal defect in computerized glow curve deconvolution of thermoluminescence. *Journal of Physics D: Applied Physics*, *34*(10), L105–L107. https://doi.org/10.1088/0022-3727/34/18/102

[48] Sakurai, T., & Gartia, R. K. (2003). Method of computerized glow curve deconvolution for analysing thermoluminescence. *Journal of Physics D: Applied Physics*, *36*(21), 2719–2724. https://doi.org/10.1088/0022-3727/36/21/020

[49] Kierstead, J., & Levy, P. (1991). Validity of repeated initial rise thermoluminescence kinetic parameter determinations. *International Journal of Radiation Applications and Instrumentation. Part D. Nuclear Tracks and Radiation Measurements*, *18*(1–2), 19–25. https://doi.org/10.1016/1359-0189(91)90087-x

[50] Bos, A., Piters, T., De Vries, W., & Hoogenboom, J. (1990). Comparative Study of Trapping Parameters of LiF (TLD-100) from Different Production Batches. *Radiation Protection Dosimetry*, *33*(1–4), 7–10. https://doi.org/10.1093/oxfordjournals.rpd.a080744

[51] Sadek, A., Abdou, N., & Alazab, H. A. (2022). Uncertainty of LiF thermoluminescence at low dose levels: Experimental results. *Applied Radiation and Isotopes*, *185*, 110245. https://doi.org/10.1016/j.apradiso.2022.110245

[52] Yasuda, H., & Fujitaka, K. (2000). Non-linearity of the high temperature peak area ratio of 6LiF:Mg,Ti (TLD-600). *Radiation Measurements*, *32*(4), 355–360. https://doi.org/10.1016/s1350-4487(00)00069-x

[53] Ajiboye, A. R., Abdullah-Arshah, R., Qin, H., & Isah-Kebbe, H. (2015). Evaluating the effect of dataset size on predictive model using supervised learning technique. *International Journal of Computer Systems & Software Engineering*, *1*(1), 75–84. https://doi.org/10.15282/ijsecs.1.2015.6.0006